Electronic supplementary information

Photodissociation processes of a water-oxygen complex cation studied by the ion imaging technique

Yuji Nakashima,[a] Yuri Ito,[a] Kenichi Okutsu,[a] Motoyoshi Nakano,[a] and Fuminori Misaizu[a*]

[a] *Department of Chemistry, Graduate School of Science, Tohoku University, 6–3 Aoba, Aramaki, Aoba-ku, Sendai 980–8578, Japan*

[*] Corresponding author: misaizu@tohoku.ac.jp

Methods

Experimental methods

In the imaging experiment, a linear-type double reflectron mass spectrometer combined with a position sensitive detector (PSD) was used, which enabled both mass selection of precursor ions and mass analysis/focused imaging of photofragment ions.[1] Details of the apparatus were already reported elsewhere.[2,3] Cluster ions including the $O_2^+(H_2O)$ precursor ion were generated by supersonic expansion and electron impact ionization methods. To obtain H_2O/O_2/He mixture gas, O_2 gas diluted with helium was passed through a reservoir containing water at 0° C. The stagnation pressure of the mixture gas was 4 atm, and the concentrations of H_2O and O_2 were 0.15% and 15%, respectively. The gas mixture was expanded into a source chamber through a pulsed valve to make a supersonic molecular beam. The molecular beam was intersected by an electron beam accelerated up to 40-45 eV to generate an ion beam containing $O_2^+(H_2O)$. The nozzle orifice of the pulsed valve was placed as close as possible to the electron beam so that the $O_2^+(H_2O)$ precursor ions could be efficiently cooled by multiple collisions in the supersonic expansion. Then the ion beam was introduced into a time-of-flight (TOF) mass spectrometer. The TOF mass spectrometer consisted of a Wiley-McLaren type acceleration region, a double reflection region, and the PSD. The cluster ions were accelerated in the acceleration region up to ca. 1 keV and injected into the double reflection region. The double reflection region was comprised of two sets of reflection electrodes (first and second reflectrons), to which synchronized pulsed high voltages were applied. The accelerated ions passed through the first reflectron (with the pulsed high voltage turned off) and were reflected by the second reflectron (turned on). As a result, the $O_2^+(H_2O)$ precursor ion was mass-separated in this region. At the middle of the two reflectrons, the precursor ion was irradiated with linearly polarized photodissociation laser. For the photodissociation laser, a third harmonic of a pulsed Nd:YAG laser (355 nm, 3.49 eV, ~60 mJ/cm^2, Spectra Physics, GCR-130) or an output from a dye laser

at 473 nm wavelength (2.62 eV, ~60 mJ/cm^2, Sirah Cobra) pumped by a third harmonic of a Nd:YAG laser (Spectra Physics, GCR-150). Coumarin 480 (Exciton, Inc.) dye was used for the dye laser. The radius of the photodissociation laser beam was ϕ2. The photodissociation laser beam was introduced into the chamber without using focusing lens. We checked the laser power dependence of the photofragment-ion intensity at 355 nm and confirmed one-photon photodissociation process. The polarization direction of the photolysis light was rotated by a Babinet–Soleil compensator (Shimadzu) and purified by a Glan-laser polarizer prism (Sigma, GLP).

The resultant photofragment ions, O_2^+ and H_2O^+, were reflected by the second reflectron (turned on), passed through the first reflectron (turned off), and flew to the PSD (Photonis, 3040FM, 60:1, ϕ40). The PSD consisted of dual-stacked microchannel plates (MCPs) and a phosphor screen (P47). Either O_2^+ or H_2O^+ photofragment ions were mass-selectively detected by the PSD by controlling the timing of gate pulse to the MCPs. Photoemission from the phosphor screen was accumulated by a charge coupled device (CCD) camera or a complementary metal oxide semiconductor (CMOS) camera. When observing the O_2^+ photofragment ions, a CCD camera (Hamamatsu, ORCA-ER, C4742-80-12AG-HEAL) was used, and a CMOS camera (Toshiba Teli, BU238M) was used for detection of H_2O^+. The use of the different cameras did not affect the experimental results. The photodissociation laser was alternately turned on and off by every 10 000 shots, and the image accumulation was performed for ca. 100 000 laser shots in total. Images of the O_2^+ and H_2O^+ photofragment ions were finally obtained by subtracting the laser-off images from the laser-on images. The slices of the three-dimensional distributions of the photofragment ions were reconstructed from the observed images by using the pBASEX method.[4] In order to convert the radii of the reconstructed images into velocity of the photofragment ion, trajectories of the ions in the experimental apparatus were simulated by the SIMION program.[5] From the results of the simulations, calibration curves were obtained which converted the radii into the velocity. The emission from the phosphor screen was also detected by a photomultiplier tube. The anode voltage of the PMT was monitored by an oscilloscope to obtain TOF spectra.

Theoretical methods

Stable structures of $O_2^+(H_2O)$ were calculated using unrestricted MP2 (UMP2) with aug-cc-pVTZ basis set of Gaussian09.[6] Charge distribution of $O_2^+(H_2O)$ was calculated by natural bond orbital (NBO) analysis. In order to determine dissociation energy of $O_2^+(H_2O)$ in the electronic ground state, D_0, geometrical optimization of O_2^+ and H_2O was also performed at UMP2/aug-cc-pVTZ. The dissociation energy was calculated by the following formula,

$$D_0 = [E(O_2^+) + E(H_2O)] - E(O_2^+(H_2O)) + [ZPE(O_2^+) + ZPE(H_2O)] - ZPE(O_2^+(H_2O)),$$

where E(M) and ZPE(M) represent total electron energy and zero-point vibrational energy of chemical species M, respectively. ZPE was calculated using harmonic frequency. In addition, geometrical optimization and vibrational frequency calculation of $O_2^+(H_2O)$ were performed under the "counterpoise"

keyword of Gaussian 09, in order to avoid overestimation of the D_0 value caused by basis set superposition error (BSSE).

Excited state calculations of $O_2^+(H_2O)$ were performed using state-averaged complete active space self-consistent field (SA-CASSCF) with MOLPRO program.[7] In the state averaging, five $^2A'$, six $^2A''$, one $^4A'$, and three $^4A''$ states were considered. Vertical excitation energy, transition dipole moment, and oscillator strength were calculated at the level of SA-CASSCF(13,11)/cc-pVTZ for the optimized structures of $O_2^+(H_2O)$. Then PECs and two-dimensional PESs of $O_2^+(H_2O)$ in the electronic ground and excited states were calculated at the same calculation level. In the calculation of the PECs, intermolecular distance between the O_2 and H_2O moieties was changed. When calculating the PESs, molecular orientations of the O_2 and H_2O units were changed. See the section of "Results and Discussion" for the details on the choice of the coordination axes for the PECs and PESs.

Supplemental figures and tables

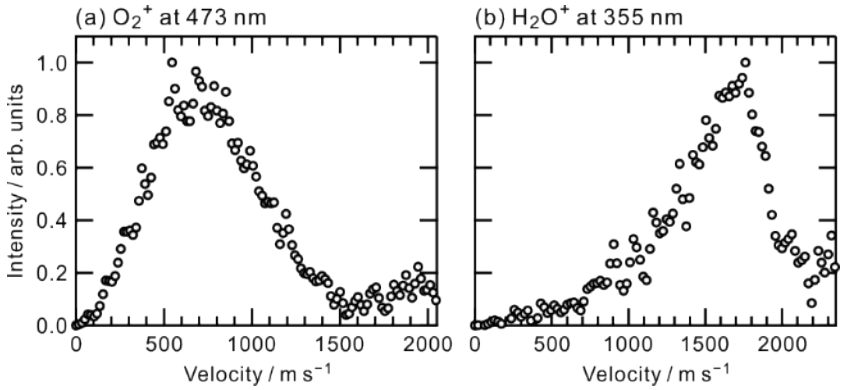

Fig. S1 The velocity distributions of the photofragment ions produced from $O_2^+(H_2O)$. (a) O_2^+ photofragment ion at 473 nm excitation. (b) H_2O^+ photofragment ion at 355 nm excitation.

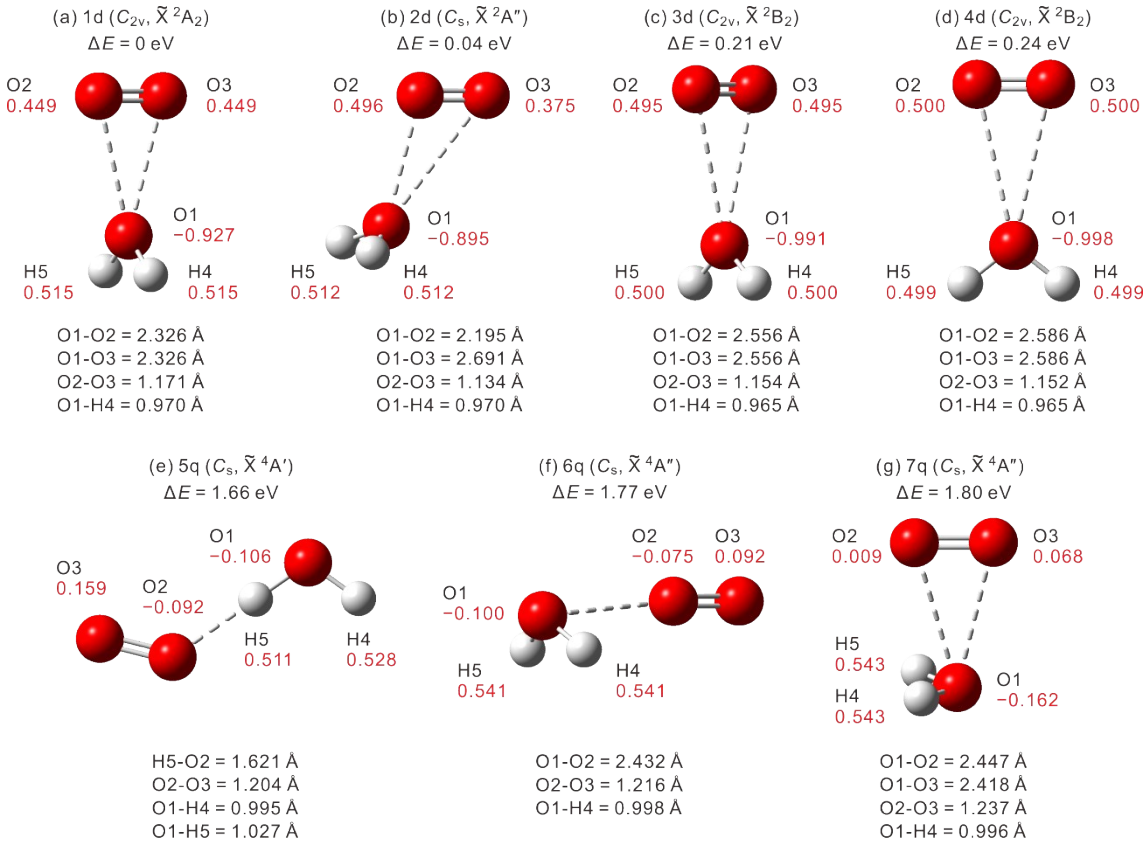

Fig. S2 Stable structures of $O_2^+(H_2O)$, 1d-4d and 5q-7q, calculated at UMP2/aug-cc-pVTZ. ΔE is the relative energy including the zero-point vibrational energy. The NBO charge of each atom in the unit of the elementary charge, *e*, is shown in red below the symbol.

Table S1 Vertical excitation wavelength, excitation energy, and oscillator strength of $O_2^+(H_2O)$ (structure 2d) calculated at SA-CASSCF(13,11)/aug-cc-pVTZ level.

Electronic states	Excitation wavelength / nm	Excitation energy / eV	Oscillator strength, f
b^4A''	314	3.95	0.000
$\tilde{E}^2A'$	322	3.85	0.000
D^2A''	411	3.02	0.098
$\tilde{C}^2A'$	418	2.97	0.000
$\tilde{B}^2A''$	544	2.28	0.104
$\tilde{a}^4A''$	688	1.80	0.000
$\tilde{A}^2A'$	2043	0.61	0.000
$\tilde{X}^2A''$	---	0.00	---

Table S2 Vertical excitation wavelength, excitation energy, and oscillator strength of $O_2^+(H_2O)$ (structure 1d) calculated at SA-CASSCF(13,11)/aug-cc-pVTZ level.

State (C_s) (C_{2v})	Excitation wavelength / nm	Excitation energy / eV	Oscillator strength, f
E^2A' ($^2B_2$)	358	3.47	0.000
b^4A'' ($^4B_1$)	405	3.06	0.000
D^2A'' ($^2A_2$)	460	2.69	0.086
C^2A' ($^2B_2$)	467	2.66	0.000
B^2A'' ($^2A_2$)	635	1.95	0.113
$\tilde{a}^4A''$ ($^4A_2$)	785	1.58	0.000
A^2A' ($^2B_2$)	2926	0.42	0.000
X^2A'' ($^2A_2$)	---	0.00	---

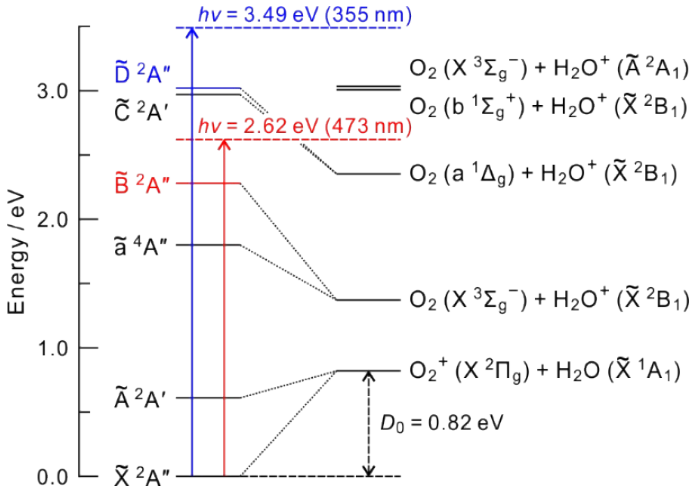

Fig. S3 Energy diagram of the electronic states of $O_2^+(H_2O)$ (structure 2d) and their dissociation limits. The dissociation limit is offset by the binding energy, D_0, of the structure 2d calculated in the present study.

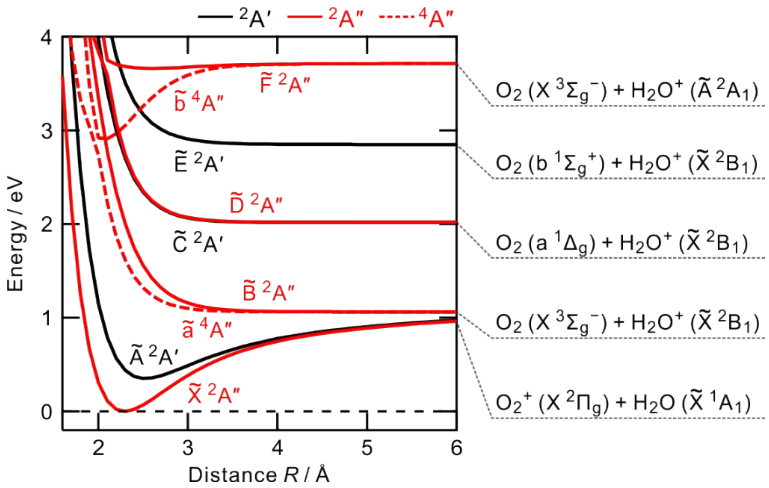

Fig. S4 PECs of the structure 1d calculated at SA-CASSCF(13,11)/aug-cc-pVTZ level. The distance R is the distance between the centers of mass of the O_2 and H_2O units of $O_2^+(H_2O)$, which was defined in Fig. 3c of the manuscript.

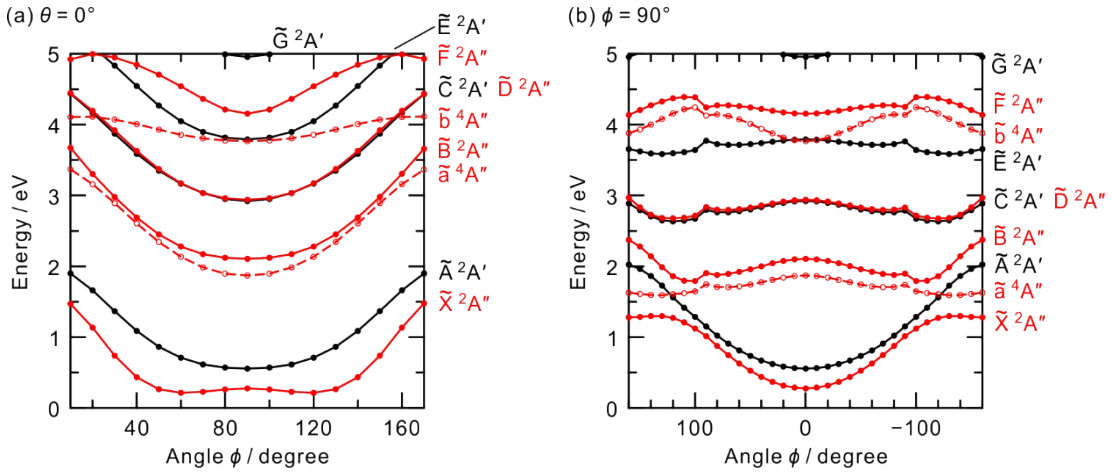

Fig. S5 Cross sectional views of the PESs (a) along θ =0° and (b) ϕ = 90° axes, calculated at SA-CASSCF(13,11)/aug-cc-pVTZ level. The original PESs were shown in Fig. 6 of the manuscript. The angles θ and ϕ represent the orientations of the H_2O and O_2 units, respectively, which were defined in Fig. 3c.

References

1 Y. Nakashima, M. Nakano, K. Okutsu, Y. Ito and F. Misaizu, *J. Phys.: Conf. Ser.*, 2020, **1412**, 132039.

2 K. Okutsu, Y. Nakashima, K. Yamazaki, K. Fujimoto, M. Nakano, K. Ohshimo and F. Misaizu, *Rev. Sci. Instrum.*, 2017, **88**, 053105.

3 Y. Nakashima, K. Okutsu, K. Fujimoto, Y. Ito, M. Kanno, M. Nakano, K. Ohshimo, H. Kono and F. Misaizu, *Phys. Chem. Chem. Phys.*, 2019, **21**, 3038.

4 G. A. Garcia, L. Nahon and I. Powis, *Rev. Sci. Instrum.*, 2004, **75**, 4989.

5 D. Manura and D. Dahl, SIMION 8.0 User Manual, Scientific Instrument Services, Inc., Ringoes, NJ 08551, 2008.

6 M. J. Frisch, Gaussian 09, Revision E.01, Gaussian, Inc., Wallingford CT, 2013.

7 H.-J.Werner, P. J. Knowles, G. Knizia, F. R. Manby, M. Schütz et al., MOLPRO, version 2015.1, a package of ab initio programs, see http://www.molpro.net.